

Achaete-scute family bHLH transcription factor 2 activation promotes hepatoblastoma progression

Yutaka Kato¹ | Takahiro Fukazawa^{2,3} | Keiji Tanimoto⁴ | Masami Kanawa² |
 Masato Kojima^{2,5,6}  | Isamu Saeki^{5,6} | Sho Kurihara^{5,6} | Ryo Touge^{5,6} |
 Nobuyuki Hirohashi⁴ | Satoshi Okada¹ | Eiso Hiyama^{2,5,6} 

¹Department of Pediatrics, Graduate School of Biomedical and Health Sciences, Hiroshima University, Hiroshima, Japan

²Natural Science Center for Basic Research and Development, Hiroshima University, Hiroshima, Japan

³Division of Medical Research Support, Advanced Research Support Center, Ehime University, Toon, Japan

⁴Department of Radiation Disaster Medicine, Research Institute for Radiation Biology and Medicine, Hiroshima University, Hiroshima, Japan

⁵Department of Surgery, Graduate School of Biomedical and Health Sciences, Hiroshima University, Hiroshima, Japan

⁶Department of Pediatric Surgery, Hiroshima University Hospital, Hiroshima, Japan

Correspondence

Eiso Hiyama, Natural Science Center for Basic Research and Development, Hiroshima University, 1-2-3 Kasumi, Minami-ku, Hiroshima 734-8551, Japan.
 Email: eiso@hiroshima-u.ac.jp

Funding information

Japan Agency for Medical Research and Development, Grant/Award Number: JP22am221403 and JP22ck0106609; Japan Society for the Promotion of Science, Grant/Award Number: JP20K08927, JP22H031315 and JP22KK0133

Abstract

Achaete-scute family bHLH transcription factor 2 (ASCL2) is highly expressed in hepatoblastoma (HB) tissues, but its role remains unclear. Thus, biological changes in the HB cell line HepG2 in response to induced ASCL2 expression were assessed. ASCL2 expression was induced in HepG2 cells using the Tet-On 3G system, which includes doxycycline. Cell viability, proliferation activity, mobility, and stemness were evaluated using 3-(4,5-dimethylthiazol-2-yl)-2,5-diphenyltetrazolium bromide, colony-formation, migration, invasion, and sphere-formation assays. Quantitative reverse-transcription polymerase chain reaction was used to assess the expression of markers for proliferation (*CCND1* and *MYC*), epithelial-mesenchymal transition (EMT; *SNAI1*, *TWIST1*, and *ZEB1*), mesenchymal-epithelial transition (*CDH1*), and stemness (*KLF4*, *POU5F1*, and *SOX9*). Compared with the non-induced HepG2 cells, cells with induced ASCL2 expression showed significant increases in viability, colony number, migration area (%), and sphere number on days 7, 14, 8, and 7, respectively, and invasion area (%) after 90 h. Furthermore, induction of ASCL2 expression significantly upregulated *CCND1*, *MYC*, *POU5F1*, *SOX9*, and *KLF4* expression on days 2, 2, 3, 3, and 5, respectively, and increased the ratios of *SNAI1*, *TWIST1*, and *ZEB1* to *CDH1* on day 5. ASCL2 promoted the formation of malignant phenotypes in HepG2 cells, which may be correlated with the upregulation of the Wnt signaling pathway-, EMT-, and stemness-related genes. ASCL2 activation may therefore be involved in the progression of HB.

KEYWORDS

basic helix–loop–helix transcription factor, growth, hepatoblastoma, phenotype, Wnt signaling pathway

This is an open access article under the terms of the [Creative Commons Attribution-NonCommercial License](https://creativecommons.org/licenses/by-nc/4.0/), which permits use, distribution and reproduction in any medium, provided the original work is properly cited and is not used for commercial purposes.

© 2024 The Authors. *Cancer Science* published by John Wiley & Sons Australia, Ltd on behalf of Japanese Cancer Association.

1 | INTRODUCTION

Hepatoblastoma (HB) is the most common malignant childhood liver tumor. Although HB is thought to be derived from hepatoblasts, which are hepatic precursor cells, its pathogenesis remains unclear.

There is a high incidence of HB in patients diagnosed with Beckwith–Wiedemann syndrome, especially in those with uniparental disomy at 11p15.5.¹ This has led to speculation that alterations in DNA methylation or genomic imprinting at 11p15.5 may be involved in HB development and progression. In our previous study, DNA methylation profiling of 163 pediatric liver tumors revealed aberrant methylation at 11p15.5, which included achaete-scute family bHLH transcription factor 2 (*ASCL2*) demethylation.² Furthermore, our previous study² showed that the transcription factor *ASCL2*, which is known to be expressed in intestinal epithelium stem cells,³ is also highly expressed in HB.² Profiling has shown that the specific hypomethylation of hepatocyte enhancers is sustained in HB, and this hypomethylation then enables these sites to bind *ASCL2*.² Upregulated *ASCL2* expression in premature hepatoblasts may therefore be associated with the development of HB.²

While *ASCL2* is known to be important in several different cancers,^{4–10} its biological functions in HB have not yet been clarified. In this study, we aimed to investigate the biological changes with induced *ASCL2* expression in the HB cell line HepG2, with the knock-down of *ASCL2* expression in the HB cell lines HepG2 and HUH-6, and with a demethylating agent in HepG2 cell lines with and without induced *ASCL2* expression, to elucidate the function of *ASCL2* in HB.

2 | MATERIALS AND METHODS

2.1 | Cell culture

The human hepatoblastoma cell lines HepG2 (Japanese Collection of Research Bioresources Cell Bank) and HUH-6 (Japanese Collection of Research Bioresources Cell Bank) were cultured in RPMI (Roswell Park Memorial Institute) 1640 with L-glutamine liquid (Nacalai Tesque) supplemented with 10% fetal bovine serum (FBS; Nacalai USA) and 100 µg/mL kanamycin (Nacalai Tesque) at 37°C in an atmosphere containing 5% CO₂. For the induced expression experiments (Tet-On 3G Systems) tetracycline-free FBS (BioWest) was used.

2.2 | Plasmids

For the induced expression experiments, complementary DNA (cDNA) encoding *ASCL2* (NCBI, CDS CCDS7732.1) was amplified by PCR using PrimeSTAR® Max DNA polymerase (Takara Bio Inc.). The amplified cDNA was cloned into a pTRE3G vector (Clontech Laboratories) using an In-Fusion Cloning Kit (Clontech), according to the manufacturer's instructions, and was subsequently referred to as pTRE *ASCL2* (Table S1). The construct was confirmed by sequencing

analysis and transiently co-transfected with the pCMV-Tet3G vector (Clontech) into HepG2 cells using TransIT-LT1 Transfection Reagent (Mirus Bio LLC), and *ASCL2* induction was tested using doxycycline (Dox; Clontech) by quantitative reverse-transcription polymerase chain reaction (qRT-PCR; Figure S1A).

2.3 | Generation of HepG2 Tet-On *ASCL2* capable of expressing *ASCL2* at high levels

To generate a Tet3G-expressing stable cell line, HepG2 cells were transfected with the pCMV-Tet3G vector using TransIT-LT1 Transfection Reagent, and stable cells were then selected with 400 µg/mL G418 (Clontech). The cells were transiently transfected with pTRE3G-Luc Control Vector (Clontech) and tested for high induction and low basal expression using luciferase activity as a reporter and the *Renilla*-luciferase vector (pRL-SV40; Promega K.K.) as the control. Clones that demonstrated ideal induction characteristics were identified, and clones expressing Tet3G were referred to as HepG2 Tet-On 3G (Figure S1B).

To generate a double-stable clone capable of high *ASCL2* induction levels, the pTRE *ASCL2* was co-transfected into HepG2 Tet-On 3G along with a linear hygromycin marker (Hyg^r; Clontech), and colonies were selected with 600 µg/mL hygromycin. The clones were tested for *ASCL2* expression in the presence and absence of Dox by qRT-PCR, and the clone that generated the highest maximal and lowest basal expression levels was chosen and referred to as HepG2 Tet-On *ASCL2* (Figure S1C). For cellular function analyses, we refer to the group treated with Dox as the Dox (+) treatment group and the untreated group as the Dox (–) treatment group.

2.4 | Minimal concentration of Dox required to induce high *ASCL2* expression in HepG2 Tet-On *ASCL2* cells

The concentration of Dox required to induce high levels of *ASCL2* expression was determined using qRT-PCR. Initially, 2 × 10⁵ HepG2 Tet-On *ASCL2* cells were seeded in five wells of a well plate (Thermo Fisher Scientific) and cultured in the presence or absence of Dox for 2 days at concentrations of 0, 62.5, 125, 250, and 500 ng/mL. The expression levels of *ASCL2* and *ACTB* were assayed across these cells by qRT-PCR, as described in the subsection on qRT-PCR.

2.5 | Small interfering RNA transfections

The small interfering RNA (siRNA) used for *ASCL2* (Bex Co., Ltd.) was si*ASCL2*, and its sequence was as follows: sense 5'-GCAAG AAGCUGAGCAAGGUtt-3' and antisense 5'-ACCUUGCUCAGCUU CUUGCTT-3'.¹¹ The si*ASCL2* and AllStars Negative Control siRNA (siNC; Qiagen NV) were transfected into cells using TransIT-X2® (Mirus) and Opti-MEM (Thermo Fisher Scientific). After siRNA

transfections, the final concentrations (FCs) of siRNAs in the media were 50 and 100 nM, for experiments with the HepG2 and HUH-6 cell lines, respectively. For qRT-PCR and cellular function analyses, we refer to the groups transfected with siNC and siASCL2 as the siNC and siASCL2 groups, respectively.

2.6 | Demethylating agent

The demethylating agent 5-aza-2'-deoxycytidine (5-aza-dC; Sigma-Aldrich) was dissolved in PBS and added to an FC of 2 μ M, as previously described.¹²⁻¹⁴ For the colony-formation assay with HepG2, we refer to the groups with added PBS and 5-aza-dC as the PBS and 5-aza-dC groups, respectively. For the colony-formation assay with HepG2 Tet-On ASCL2, we refer to the Dox (-) and Dox (+) treatment groups with added PBS or 5-aza-dC as the Dox (-) & PBS, Dox (-) & 5-aza-dC, Dox (+) & PBS, and Dox (+) & 5-aza-dC groups, respectively.

2.7 | Sampling

For the induced expression experiments, 5×10^5 HepG2 Tet-On ASCL2 cells were seeded into 100-mm dishes (Thermo Fisher Scientific) and treated with Dox, and the remaining untreated cells were used as the sample on day 0 (before the Dox treatment). The cells were cultured for 1-5 days and sampled daily (Figure S2A). Half of each sample was then used for western blot analysis of ASCL2 and the other half for qRT-PCR analysis of ASCL2 and other genes of interest.

For the knockdown experiment, 2×10^5 HepG2 and HUH-6 cells, each were seeded into 2 mL of RPMI medium, as previously described in the Cell culture subsection, in 35-mm dishes (Corning Inc.) and cultured for 1 day. The siRNA complexes were then distributed to the cells (HepG2 and HUH-6; TransIT-X2® 7.5 μ L; siRNA [20 μ M stock concentration] 5.65 and 11.3 μ L; Opti-MEM 250 μ L; FC 50 and 100 nM), and the cells were cultured for 1 day, then sampled (Figure S2B,C).

2.8 | Quantitative reverse-transcription polymerase chain reaction

Total RNA was isolated from the cells using NucleoSpin® RNA (MACHEREY-NAGEL GmbH & Co. KG) or NucleoSpin® miRNA (MACHEREY-NAGEL GmbH & Co. KG) kits, according to the manufacturer's instructions. The isolated RNA was quantified using a NanoDrop 1000 spectrophotometer (Thermo Fisher Scientific). Total RNA extracted from each sample was diluted to 1000 ng/10 μ L (FC of 100 ng/ μ L), and cDNA was synthesized using a High-Capacity cDNA Reverse Transcription Kit (Applied Biosystems), according to the manufacturer's instructions. cDNA was diluted by five- or 20-fold (five-fold for ASCL2, 20-fold for genes of interest), and 2 μ L

of diluted cDNA was used as a template. Quantitative reverse-transcription polymerase chain reaction was performed with a FastStart Universal Probe Master (Rox; Hoffmann-La Roche Ltd), primers, and Universal ProbeLibrary Set (Roche) using a 7900HT Fast Real-Time PCR System (Applied Biosystems), 7500 Real-Time PCR System (Applied Biosystems), or CFX Opus 96 Real-Time PCR system (Bio-Rad Laboratories, Inc.). The ASCL2, CCND1, MYC, SNAI1, TWIST1, ZEB1, CDH1, KLF4, POU5F1, SOX9, and DLK1 primer and probe sets are listed in Table S2. TaqMan™ Gene Expression Assays (Applied Biosystems) were conducted using the MEG3 and RTL1 primer and probe sets, respectively. ACTB (Applied Biosystems) was used as the internal control. Gene expression levels were calculated using standard curves generated from serial dilutions of pooled cDNA from various cell lines, as previously described.¹⁵ Overall, there were four biological replicates for each sample (four different plates for each condition) and each of these was used for three technical replicates in a 96-well plate (three different wells), resulting in 12 data points per sample. For the induced expression experiments, the ratios of ASCL2, CCND1, MYC, SNAI1, TWIST1, ZEB1, CDH1, KLF4, POU5F1, SOX9, DLK1, MEG3, and RTL1 to ACTB and SNAI1, TWIST1, and ZEB1 to CDH1 were calculated, and the results for each time point were compared with those for all other time points. As the SNAI1, TWIST1, ZEB1 (epithelial-mesenchymal transition [EMT] markers), and CDH1 (mesenchymal-epithelial transition [MET] marker) combination may be used to distinguish the mesenchymal cell phenotype from the epithelial cell phenotype,¹⁶ the expression ratios of these EMT markers to CDH1 were calculated. For the knockdown experiments, the ratios of ASCL2, POU5F1, SOX9, ZEB1, and MYC to ACTB were calculated, and the HepG2 and HUH-6 cells transfected with siNC were compared to their respective counterparts transfected with siASCL2.

2.9 | Western blotting

Cells were washed with ice-cold PBS, harvested, and frozen at -80°C. Whole-cell extracts were prepared from frozen cells and their concentrations were measured as previously described.¹⁷ Each protein sample (40 μ g) was separated using 5%-10% gradient sodium dodecyl sulfate-polyacrylamide gel electrophoresis (Atto Corporation) and blotted onto polyvinylidene fluoride membranes (Millipore Corporation). To block nonspecific antibody binding, membranes were incubated with 2% bovine serum albumin in Tris-buffered saline for 1 h at room temperature (20°C). The membranes were incubated with primary antibodies diluted in CanGet Signal primary buffer (Toyobo Co., Ltd.) overnight at 4°C. The primary antibodies and their dilutions were as follows: anti-ASCL2 (Sigma-Aldrich), 1:500, and anti- β -actin (Sigma-Aldrich), 1:5000. After washing with Tris-buffered saline (pH 7.6) containing 0.05% Tween 20, membranes were incubated with horseradish peroxidase-linked anti-rabbit IgG (Cell Signaling Technology, Inc.) or anti-mouse IgG (Cell Signaling Technology) diluted in CanGet Signal secondary antibody buffer at 37°C. After washing with Tris-buffered saline (pH 7.6)

containing 0.05% Tween 20, the membranes were incubated with SuperSignal™ West Femto Maximum Sensitivity Substrate (Thermo Fisher Scientific), and the immune complexes were detected using Fujifilm Super RX X-ray film (Fujifilm) and autoradiography. Experiments were independently performed at least three times.

2.10 | 3-(4,5-dimethylthiazol-2-yl)-2,5-diphenyltetrazolium bromide assay

Cell viability was evaluated using the 3-(4,5-dimethylthiazol-2-yl)-2,5-diphenyltetrazolium bromide (MTT) assay. For the induced expression experiment, HepG2 Tet-On ASCL2 cells were cultured for 5 days with or without Dox. Cells were re-treated with or without Dox and seeded in 96-well plates (5×10^3 cells/well, eight wells \times four plates; Thermo Fisher Scientific). For the knockdown experiments, HepG2 and HUH-6 cells were seeded in 96-well plates (5×10^3 and 8×10^3 cells/well, four wells \times four plates). The cells were cultured for 1 day and then transfected with siRNA. At each time point (HepG2 Tet-On ASCL2, and cells transfected with siRNA, days 1, 3, 5, and 7, and days 1, 2, 3, and 4 [culture period after seeding in the 96-well plate]), 10 μ L of 0.4% MTT reagent and 0.1 M sodium succinate were added to each well. After 2 h of incubation, the formazan precipitates were dissolved in 150 μ L of dimethyl sulfoxide and the absorbance at 570 and 650 nm was measured using an EMax® Endpoint ELISA Microplate Reader (Molecular Devices LLC; Figure S3A–C). The relative cell viabilities were calculated using the absorbances at 570 and 650 nm at the time points mentioned, and the fold change was calculated relative to the viabilities on day 1 (i.e., on day 1 the relative cell viability showed a 1-fold increase).

2.11 | Colony-formation assay

Colony-formation ability was evaluated as follows. For the induced expression experiment, 1×10^4 HepG2 Tet-On ASCL2 cells/well were seeded in six-well plates with or without Dox and cultured for 14 days. For the knockdown experiment, HepG2 and HUH-6 cells were seeded in 96-well plates (1×10^3 and 8×10^3 cells/well). The cells were cultured for 1 day and then transfected with siRNA. The cells were then cultured for 2 days, after which cells from each of the 96 wells were seeded into a well in a six-well plate and cultured for 10 days. For the experiments using 5-aza-dC, HepG2 and HepG2 Tet-On ASCL2 cells were seeded in six-well plates (2.5×10^4 and 3.75×10^4 cells/well), and HepG2 Tet-On ASCL2 cells were treated with or without Dox. The cells were cultured for 1 day and then PBS or 5-aza-dC was added. Then, 2 and 4 days after first adding the PBS or 5-aza-dC, the media were changed and PBS or 5-aza-dC was added. The cells were then cultured for 7 days after seeding. Cells were fixed with ice-cold 100% methanol, stained with 0.5% crystal violet, and examined using a scanner (DS-7500; Seiko Epson Corporation; Figure S4A–E). Visible colonies in the culture were counted using Katikati counter software (<https://www.vector.co.jp/>

[soft/win95/art/se347447.html](https://www.vector.co.jp/soft/win95/art/se347447.html); Figure S4F), and the Dox (–) treatment, siNC, and PBS groups were compared with the Dox (+) treatment, siASCL2, and 5-aza-dC groups on days 14, 10, and 7 of the culture period after seeding in a six-well plate (Figure S4A–D). For the experiments using HepG2 Tet-On ASCL2 and 5-aza-dC, one particular group was compared with all other groups on day 7 of the culture period (Figure S4E).

2.12 | Migration assay

Standardized wounds for the migration assay were created using Culture-Insert 2 Wells (ibidi GmbH). Briefly, for the induced expression experiment, HepG2 Tet-On ASCL2 cells were cultured for 5 days with or without Dox before seeding into the wells (migration-day [M-day: culture period after removing the Culture-Insert 2 Well] – 1 = day [culture period after the Dox (–) and (+) treatment] 5). The cells were seeded into each well (14×10^4 cells/70 μ L medium with or without Dox, M-day – 1 = day 5) and cultured for 1 day. The Culture-Insert 2 Wells were then gently removed, and the medium with or without Dox was added (M-day 0 [migration assay start] = day 6; Figure S5A). For the knockdown experiment, HepG2 and HUH-6 cells were seeded into each well (15×10^3 cells/60 μ L medium, respectively) and cultured for 1 day. The cells were then transfected with siRNA and cultured for 2 days. The Culture-Insert 2 Wells were then gently removed, and RPMI medium, as previously described in the Cell culture subsection, was added (Figure S5B,C). Cells were cultured and photographed at the indicated time points (HepG2 Tet-On ASCL2 and HepG2 transfected with siRNA: days 2 and 4; HUH-6 transfected with siRNA: 24, 36, and 48 h of the culture period after removing the Culture-Insert 2 Wells) using a Leica DMI1 (Leica Microsystems CMS GmbH; Figure S5A–C). The migration abilities were compared at the time points mentioned by calculating the migration areas using ImageJ software (public domain open-source software, imagej.nih.gov), as previously described¹⁸ (Figure S5D).

2.13 | Invasion assay

The invasion assay was performed according to a previously described method with slight modifications.¹⁹ For the induced expression experiment, HepG2 Tet-On ASCL2 cells were cultured for 3 days with or without Dox before being used in a hanging-drop culture. To form spheroids, the cells were cultured using the hanging-drop method for 2 days (2.0×10^4 cells/20 μ L medium with or without Dox). For the knockdown experiment, HepG2 cells were cultured using the hanging-drop method, and after 1 day, the drops were transfected with siRNA. The drops were then cultured for 2 days after the siRNA transfections. The spheroids formed were embedded in 500 μ L of collagen I solution (350 μ L of Cellmatrix Type I-A [FUJIFILM Wako Pure Chemical Corporation], 100 μ L of medium, and 50 μ L of Reconstitution Buffer [FUJIFILM Wako Pure Chemical Corporation], mixed on ice) in each well of a 24-well plate

and incubated for 10 min at 37°C. Serum-free medium (500 μ L) was added on top of the solidified collagen I, and the spheroids were photographed after being embedded in collagen I and incubated for 0, 5, 10, 30, 50, and 90 h (HepG2 Tet-On ASCL2) or 2, 4, and 6 days (HepG2 transfected with siRNA), with an All-in-One Fluorescence Microscope BZ-X800 (KEYENCE Corporation; Figure S6A,B). The same coordinates (*x*, *y*, and *z* axes) were used for each well, and the invasion abilities were compared at the time points mentioned by calculating the invasion areas using ImageJ software (Figure S6C).

2.14 | Sphere-formation assay

For the induced expression experiment, HepG2 Tet-On ASCL2 cells (5×10^4) were cultured with or without Dox after seeding on $\varphi 90 \times 20$ mm Asnol Petri dishes (AS ONE Corporation) for 7 days (Figure S7A). For the knockdown experiment, 2×10^3 HepG2 cells/well were seeded in a 96-well plate. The cells were cultured for 1 day and then transfected with siRNA. The cells were cultured for 2 days after the siRNA transfections, then cells from each of the 96 wells were seeded on an Asnol Petri dish and cultured for 10 days (Figure S7B). Spheres were scanned with a scanner (DS-7500) and photographed with a Leica DMI1, and visible spheres were counted using the Katikati counter software. The Dox (-) treatment and the siNC groups were compared with the Dox (+) treatment and siASCL2 groups on day 7 or 10 of the culture period after seeding in an Asnol Petri dish (Figure S7C).

2.15 | Statistical analyses

Statistical analyses were performed using SPSS Statistics version 17.0 (IBM). For comparisons involving more than three groups, one-way ANOVA was used, and the Games–Howell and Tukey tests were used to compare the expression of each gene at a particular time point with that at all other measured time points in the qRT-PCR analysis for HepG2 Tet-on ASCL2 and to compare the colony number of a particular group with that of all other groups in the colony-formation assay using HepG2 Tet-On ASCL2 and 5-aza-dC. For cellular function analyses, the Dox (-) and Dox (+) groups and the siNC and siASCL2 groups were compared using Student's *t*-test. Statistical significance was set at $P < 0.05$.

3 | RESULTS

3.1 | Minimal concentration of Dox required to induce high ASCL2 expression in HepG2 Tet-On ASCL2 cells

A stable clone in which high ASCL2 induction could be achieved using Dox, HepG2 Tet-On ASCL2, was created using the Tet-On 3G system. The HepG2 Tet-On ASCL2 cells were cultured with 0, 62.5, 125,

250, and 500 ng/mL Dox, and the expression levels of ASCL2/ACTB were 0.07 (0.01), 14.32 (0.75), 14.30 (0.64), 21.02 (2.30), and 20.25 (1.28), respectively (mean [SD], $n = 3$). In the cells treated with lowest concentration of Dox (62.5 ng/mL), the ASCL2/ACTB expression level was found to be sufficiently high to enable investigations into the associated biological effects, when compared with the Dox (-) treatment group. Thus, the minimal concentration of Dox required to induce high expression was determined to be 62.5 ng/mL (Figure S8).

3.2 | ASCL2 expression induced by Dox

In HepG2 Tet-On ASCL2 cells cultured in the presence of Dox, the expression levels of ASCL2/ACTB on days 1, 2, 3, 4, and 5 (culture period after the Dox treatment) were found to be 384.8 (76.3), 529.9 (104.7), 635.5 (202.2), 860.7 (248.1), and 2765.2 (609.6), respectively (mean [SD], $n = 4$); these levels were remarkably higher than those on day 0, before the Dox treatment (1.0 [0.7], mean [SD], $n = 4$; Figure S9A).

Western blotting showed that the ASCL2 protein levels gradually increased from day 0 to day 4 (culture period after the Dox treatment) and then markedly increased on day 5, similar to the ASCL2 messenger RNA expression on day 5 (Figure S9B).

3.3 | ASCL2 knockdown by siRNA

In HepG2 and HUH-6 transfected with siRNAs, the expression levels of ASCL2/ACTB were significantly lower in the siASCL2 group than in the siNC group (mean [SD] 0.60 [0.42] vs. 1.68 [0.68] and 0.62 [0.23] vs. 1.51 [0.50], $P = 0.036$ and 0.017 , $n = 4$; Figure S10A,B).

3.4 | MTT and colony-formation assays

In the MTT assay with HepG2 Tet-On ASCL2, on day 7, relative cell viability when compared with that on day 1 was significantly higher with the Dox (+) treatment than with the Dox (-) treatment (mean [SD] 18.29 [0.94]-fold vs. 13.25 [1.29]-fold, $P < 0.001$, $n = 4$; Figure 1A). In HepG2 transfected with siRNAs, on day 4, the cell viability was significantly lower with siASCL2 transfection than with siNC transfection (mean [SD] 6.74 [0.50]-fold vs. 8.49 [0.92]-fold, $P = 0.016$, $n = 4$; Figure S11A). In HUH-6, cell viabilities with siASCL2 transfection were also significantly lower from days 2 to 4 (mean [SD] 1.12 [0.08]-fold vs. 1.66 [0.15]-fold, 0.93 [0.16]-fold vs. 1.99 [0.10]-fold, and 1.10 [0.17]-fold vs. 2.55 [0.10]-fold, $P = 0.002$, < 0.001 , and < 0.001 , respectively, $n = 4$; Figure S11B).

For the HepG2 Tet-On ASCL2, the results of the colony-formation assay showed that both colony number (Figure 1B) and size (Figure 1C) were greater in the Dox (+) treatment group than in the Dox (-) treatment group (on day 14, mean [SD] 76.5 [9.0] colonies vs. 24.5 [4.3] colonies, $P < 0.001$, $n = 6$). In HepG2 and HUH-6, the results of the colony-formation assay showed that

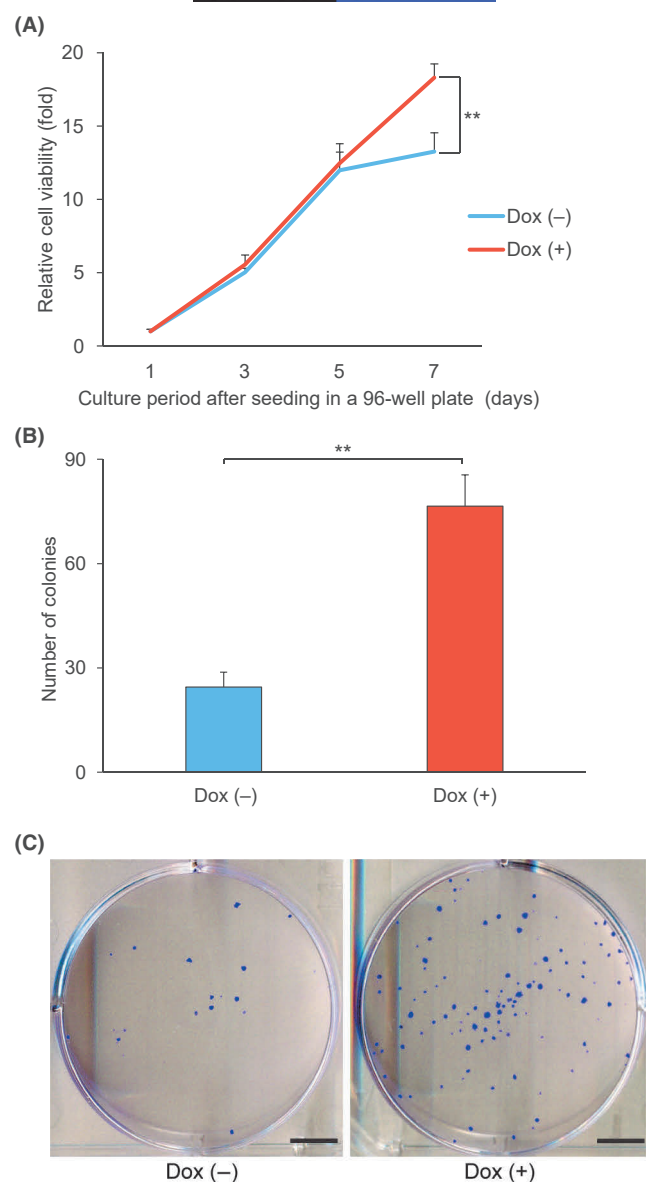


FIGURE 1 MTT and colony-formation assays in the induced expression experiment using HepG2 Tet-On ASCL2. (A) HepG2 Tet-On ASCL2 cell viability was evaluated using an MTT assay. The relative cell viabilities were calculated using the absorbances at 570 and 650 nm at the indicated time points (days 3, 5, and 7), and the fold change was calculated relative to the viabilities on day 1. On day 7, cell viability was significantly higher with the Dox (+) treatment than with the Dox (-) treatment (relative cell viability [fold], mean [SD] 18.29 [0.94]-fold vs. 13.25 [1.29]-fold, $P < 0.001$, $n = 4$). Days 1, 3, 5, and 7 refer to the culture period after seeding in the 96-well plate. Values shown are the means \pm SD. $**P < 0.01$. Cells were seeded in eight wells of a 96-well plate in four plates for each group. (B) Colony-forming abilities were evaluated using a colony-formation assay with the HepG2 Tet-On ASCL2 cells. The number of colonies was greater with the Dox (+) treatment than with the Dox (-) treatment (on day 14, mean [SD] 76.5 [9.0] colonies vs. 24.5 [4.3] colonies, $P < 0.001$, $n = 6$). Seeding in a six-well plate was also carried out on day 0 of the culture period after the Dox treatment. Values shown are the means \pm SD. $**P < 0.01$. (C) Representative images of the Dox (-) and (+) treatments groups on day 14. Colony sizes were larger with the Dox (+) treatment than with the Dox (-) treatment. Scale bar = 5 mm. Dox, doxycycline; MTT, 3-(4,5-dimethylthiazol-2-yl)-2,5-diphenyltetrazolium bromide.

were greater in the Dox (+) & 5-aza-dC group than in the Dox (-) & 5-aza-dC group.

3.5 | Migration and invasion assays

For the HepG2 Tet-On ASCL2, the migration areas (%) on M-day 2 (day 8) were significantly larger in the Dox (+) group than in the Dox (-) group (mean [SD] 33.2 [7.4]% vs. 14.1 [1.6]%, $P = 0.012$, $n = 4$; Figure 2B). Furthermore, cell shape changes, such as invadopodia, were observed in the Dox (+) group when compared with the Dox (-) group on M-day 2 (day 8; Figure 2A). In HepG2, the migration areas (%) on days 2 and 4 were significantly smaller in the siASCL2 group than in the siNC group (mean [SD] 23.9 [2.1]% vs. 35.8 [3.7]% and 57.6 [5.3]% vs. 68.3 [6.8]%, $P = 0.001$ and 0.049 , $n = 4$; Figure S14A,B). In HUH-6, the migration areas (%) at 24, 36, and 48 h were significantly smaller in the siASCL2 group than in the siNC group (mean [SD] 10.9 [5.1]% vs. 27.2 [5.1]%, 20.7 [8.5]% vs. 41.3 [9.3]%, and 32.0 [10.0]% vs. 58.4 [4.5]%, $P = 0.004$, 0.017 , and 0.003 , respectively, $n = 4$; Figure S14C,D).

For the HepG2 Tet-On ASCL2, invasion in the Dox (+) group was detected at 5 h, and the invasion areas (%) were significantly larger in the Dox (+) group than in the Dox (-) group at 30, 50, and 90 h (mean [SD] 110.0 [4.9]% vs. 98.9 [6.0]%, 112.7 [5.3]% vs. 99.0 [6.71]%, and 119.0 [6.0]% vs. 101.6 [7.2]%, $P = 0.028$, 0.019 , and 0.009 , respectively, $n = 4$; Figure 2D). Morphological changes, such as invadopodia, were observed in the Dox (+) group when compared with the Dox (-) group after 30 h (Figure 2C). In HepG2, the invasion areas (%) were significantly smaller in the siASCL2 group than in the siNC group on days 4 and 6 (mean [SD] 98.1 [1.7]% vs. 103.8 [3.9]% and 100.3 [1.3]% vs. 109.5 [6.8]%, $P = 0.036$ and 0.036 , $n = 4$; Figure S14E,F).

both colony number (Figure S11C,E) and size (Figure S11D,F) were smaller in the siASCL2 group than in the siNC group (on day 10, mean [SD] 14.3 [8.6] colonies vs. 105.5 [13.0] colonies and 194.8 [38.4] colonies vs. 331.0 [92.1] colonies, $P < 0.001$ and $P = 0.034$, $n = 4$). For the assay using HepG2 and 5-aza-dC, the colony number was 65.7% smaller in the 5-aza-dC group than in the PBS group (on day 7, mean [SD] 878.5 [24.1] colonies vs. 2558.8 [334.6] colonies, $P < 0.001$, $n = 4$, Figure S12A), and the size (Figure S12B) and number of cells forming clusters (Figure S12C) were also smaller. For the assay using HepG2 Tet-On ASCL2 and 5-aza-dC, the colony number was greater in the Dox (+) & 5-aza-dC group than in the Dox (-) & 5-aza-dC group (on day 7, mean [SD] 400.5 [36.6] colonies vs. 227.5 [76.1] colonies, $P = 0.020$, $n = 4$). Compared with the respective PBS groups, the colony number was 32.8% smaller in the Dox (+) & 5-aza-dC group, while it was 52.7% smaller in the Dox (-) & 5-aza-dC group (Figure S13A). Colony size (Figure S13B) and the number of clustering and stratifying cells (Figure S13C)

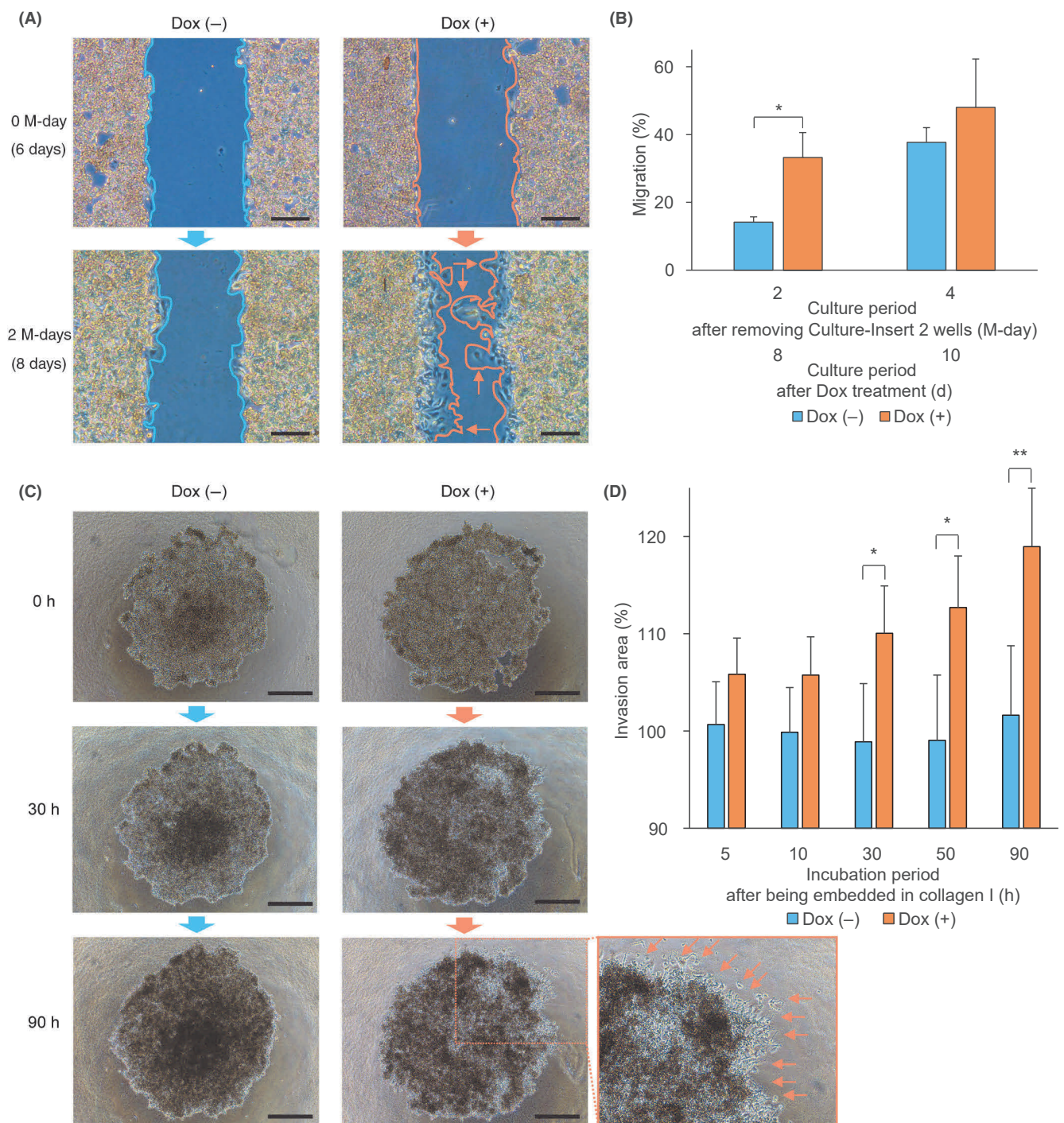


FIGURE 2 Migration and invasion assays in the induced expression experiment with HepG2 Tet-On ASCL2. (A) Representative images of the HepG2 Tet-On ASCL2 cells from the Dox (-) and (+) treatment groups that were analyzed using a migration assay. Image of the Dox (+) treatment group on M-day 2 (day 8) shows invadopodia (identified using arrows). Scale bar = 200 μ m. (B) Migration areas (%) on M-days 2 and 4 (days 8 and 10). The migration areas (%) on M-day 2 (day 8) were significantly larger with the Dox (+) treatment than with the Dox (-) treatment (mean [SD] 33.2 [7.4]% vs. 14.1 [1.6]%, respectively, $P=0.012$, $n=4$). M-days 2 and 4 refer to the culture period after removing the Culture-Insert 2 Well; days 8 and 10 refer to the culture period after the Dox (-) and (+) treatment. Values shown are the means \pm SD. * $P<0.05$. (C) Representative images of the HepG2 Tet-On ASCL2 cells from the Dox (-) and (+) treatment groups that were analyzed using an invasion assay. The image of the Dox (+) treatment group at 90h shows invadopodia, identified using arrows. Scale bar = 500 μ m. (D) Invasion areas (%) at 5, 10, 30, 50, and 90h. The invasion areas (%) at 30, 50, and 90h were significantly larger with the Dox (+) treatment than with the Dox (-) treatment (mean [SD] 110.0 [4.9]% vs. 98.9 [6.0]%, 112.7 [5.3]% vs. 99.0 [6.71]%, and 119.0 [6.0]% vs. 101.6 [7.2]%, $P=0.028$, 0.019, and 0.009, respectively). 5, 10, 30, 50, and 90h refer to the incubation period after being embedded in collagen I. Values shown are the means \pm SD ($n=4$). * $P<0.05$, ** $P<0.01$. Dox, doxycycline; M-day, migration-day.

3.6 | Sphere-formation assay

For the HepG2 Tet-On ASCL2, the number of spheres was higher in the Dox (+) group than in the Dox (-) group (on day 7, mean [SD] 515.0 [63.1] spheres vs. 412.8 [44.4] spheres, $P=0.038$, $n=4$; Figure 3B). Furthermore, the sphere sizes in the Dox (+) group were larger than those in the Dox (-) group on day 7 (Figure 3A). In HepG2, the number of spheres was smaller in the siASCL2 group than in the siNC group (on day 10, mean [SD] 147.5 [31.0] spheres vs. 274.0 [97.1] spheres, $P=0.048$, $n=4$; Figure S15B). Furthermore, the sphere sizes in the siASCL2 group were smaller than those in the siNC group on day 10 (Figure S15A).

3.7 | Gene expression before and after ASCL2 induction and during ASCL2 knockdown

The expression of *CCND1* and *MYC* significantly increased on days 2–3 and 2–4 in the HepG2 Tet-On ASCL2 cells cultured in the presence of Dox when compared with the expression on day 0 (*CCND1/ACTB*, on days 2 and 3, mean [SD] 6.95 [1.69] and 6.85 [2.42], $P=0.016$ and 0.020 , respectively, $n=4$; *MYC/ACTB*, on days 2,

3, and 4, mean [SD] 9.14 [2.73], 8.84 [3.16], and 8.28 [2.19], $P=0.006$, 0.009 , and 0.019 , respectively, $n=4$). From day 4, these levels decreased, but they were not statistically significant when compared to the levels on day 3 (*CCND1/ACTB*, *MYC/ACTB*, on days 4 and 5, mean [SD] 5.55 [1.54] and 3.74 [0.34], 8.28 [2.19] and 6.09 [0.75], $P=0.82$ and 0.080 , 1.00 and 0.46 , respectively, $n=4$; Figure 4A).

Compared with day 0, the expression ratios of *SNAI1*, *TWIST1*, and *ZEB1* (EMT markers) to *CDH1* (MET marker) were not significantly different until day 4 and were significantly increased on day 5 in HepG2 Tet-On ASCL2 cells cultured in the presence of Dox (*SNAI1/CDH1*, *TWIST1/CDH1*, and *ZEB1/CDH1*, mean [SD] 8.95 [0.69], 0.18 [0.04], and 9.67 [1.66], $P<0.001$, <0.001 , and <0.001 , respectively, $n=4$; Figures 4B and S16).

Compared with those on day 0, the expression levels of *POU5F1* and *SOX9* were significantly increased in the HepG2 Tet-On ASCL2 cells cultured in the presence of Dox on days 1–5 and 1–4 (*POU5F1/ACTB*, on days 1, 2, 3, 4, and 5, mean [SD] 4.62 [0.81], 5.42 [1.32], 6.10 [1.43], 6.54 [0.55], and 5.39 [0.13], $P=0.039$, 0.003 , <0.001 , <0.001 , and 0.003 , $n=4$, respectively, and *SOX9/ACTB*, on days 1, 2, 3, and 4, mean [SD] 4.58 [1.04], 5.28 [1.02], 5.77 [1.42], and 5.65 [0.98], $P=0.044$, 0.005 , 0.001 , and 0.002 , $n=4$, respectively), while the levels of *KLF4* significantly increased only on day 5 (*KLF4/ACTB*, mean [SD] 1.21 [0.27], $P\leq 0.001$, $n=4$; Figure 4C).

The expression of *MEG3* was significantly increased on day 5 in HepG2 Tet-On ASCL2 cells cultured in the presence of Dox when compared with that on day 0 (*MEG3/ACTB*, mean [SD] 0.023 [0.005], $P=0.004$, $n=4$; Figure S17B), while the expression of *DLK1* and *RTL1* was not significantly different (Figure S17A,C).

In HepG2, the expression of *POU5F1/ACTB* was significantly lower in the siASCL2 group than in the siNC group (mean [SD] 1.04 [0.08] vs. 1.24 [0.07], $P=0.011$, $n=4$; Figure S18A). The expression of *SOX9/ACTB* was also lower in the siASCL2 group than in the siNC group (mean [SD] 1.76 [0.15] vs. 1.94 [0.14], $P=0.13$, $n=4$; Figure S18B), although the difference was not statistically significant. There was no significant difference between the siASCL2 and siNC groups in terms of *ZEB1* and *MYC* expression (*ZEB1/ACTB* and *MYC/ACTB*, mean [SD] 1.81 [0.17] vs. 1.86 [0.15] and 1.69 [0.08] vs. 1.65 [0.03], $P=0.70$ and 0.49 , $n=4$; Figure S18C,D). In HUH-6, the expression of *POU5F1/ACTB* was also lower in the siASCL2 group than in the siNC group (mean [SD] 12.2 [3.7] vs. 14.2 [4.9], $P=0.55$, $n=4$; Figure S18E), although the difference was not statistically significant. There was no significant difference between the siASCL2 and siNC groups in terms of *SOX9*, *ZEB1*, and *MYC* expression (*SOX9/ACTB*, *ZEB1/ACTB*, and *MYC/ACTB*, mean [SD] 0.94 [0.04] vs. 0.96 [0.04], 0.085 [0.041] vs. 0.081 [0.032], and 1.56 [0.07] vs. 1.43 [0.09]; $P=0.59$, 0.90 , and 0.054 , respectively, $n=4$; Figure S18F–H).

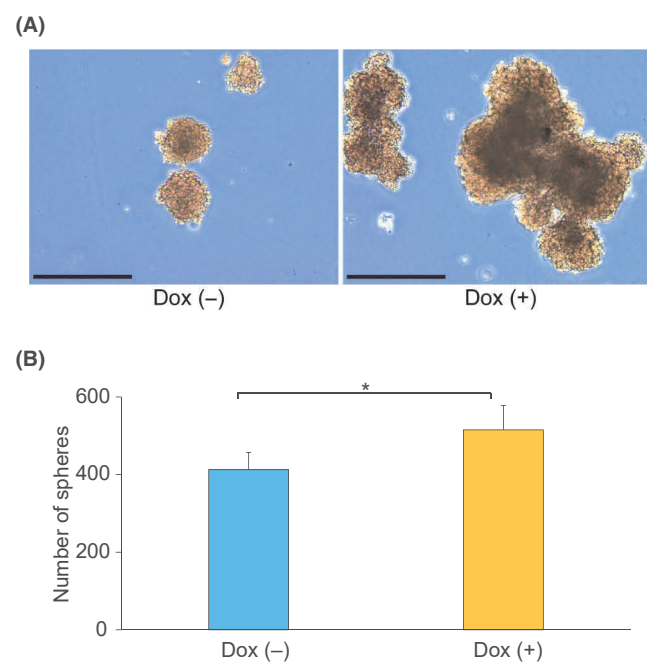


FIGURE 3 Sphere-formation assay in the induced expression experiment with HepG2 Tet-On ASCL2. (A) Representative images from the sphere-formation assay using the HepG2 Tet-On ASCL2 cells from the Dox (-) and Dox (+) treatment groups on day 7. Sphere sizes were larger with the Dox (+) treatment than with the Dox (-) treatment. Scale bar = 0.5 mm. (B) Sphere-formation abilities of the HepG2 Tet-On ASCL2 cells were evaluated on day 7 using the sphere-formation assay. There were more spheres with the Dox (+) treatment than with the Dox (-) treatment (mean [SD] 515.0 [63.1] spheres vs. 412.8 [44.4] spheres, $P=0.038$, $n=4$). Day 7: culture period after seeding in an Asnol Petri dish. Values shown are the means \pm SD. * $P<0.05$. Dox, doxycycline.

4 | DISCUSSION

In HepG2 cells, increased ASCL2 expression was found to promote malignant phenotypes, including growth, mobility, and stemness (Figure S19). MTT and colony-formation assays were conducted to

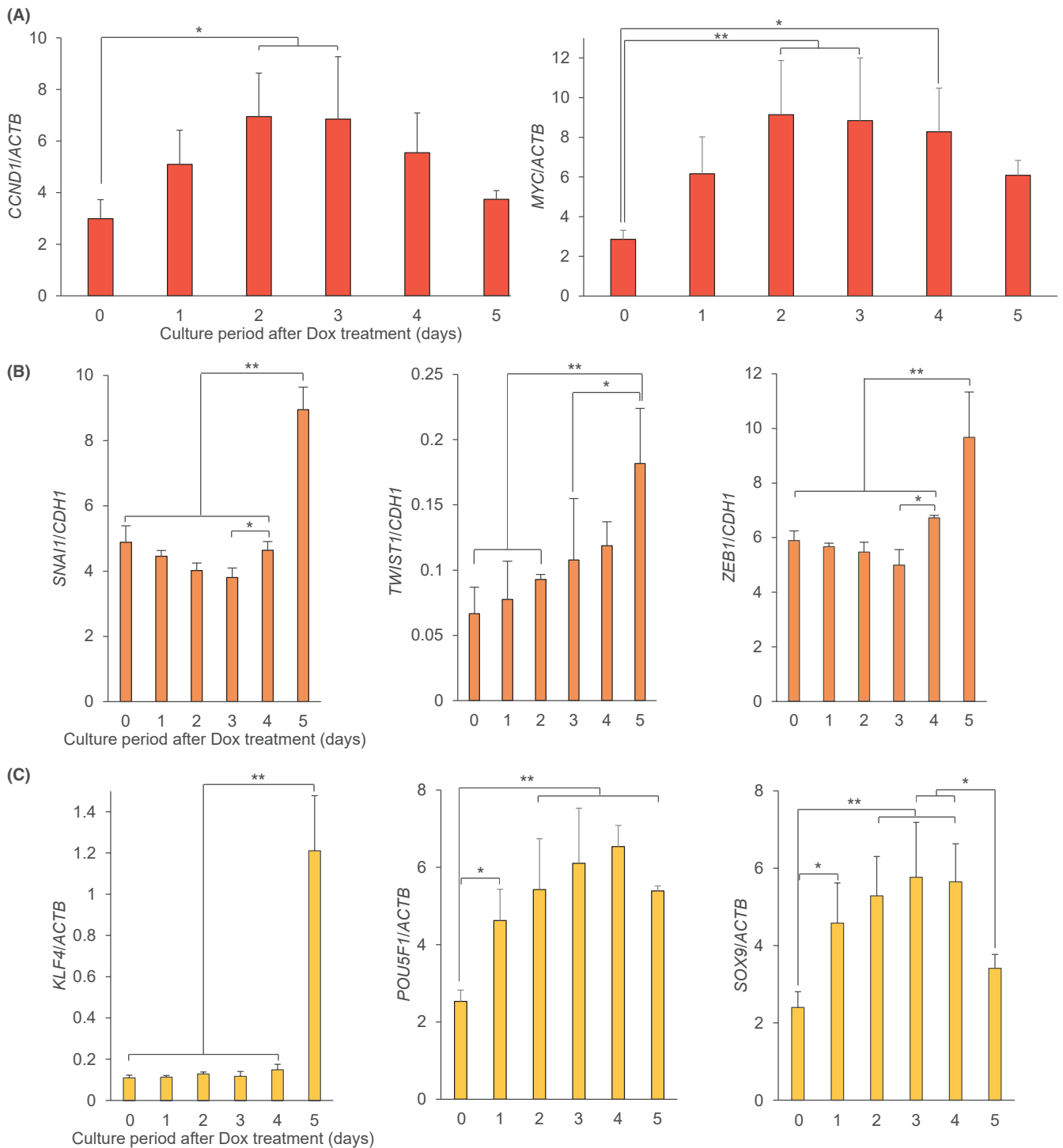


FIGURE 4 Expression of proliferation-, EMT-, and stemness-related genes before and after the induction of ASCL2. (A) *CCND1* and *MYC* (proliferation markers)/*ACTB* expression levels. The levels of *CCND1* and *MYC* significantly increased on days 2–3 and 2–4 when compared with those on day 0. Their levels decreased from day 4, although the decreases were not statistically significant when compared with those on day 3. (B) *SNAI1*, *TWIST1*, and *ZEB1* (EMT markers)/*CDH1* (a MET marker) expression ratios. Compared with day 0, the ratios of *SNAI1*, *TWIST1*, and *ZEB1* to *CDH1* were not significantly different until day 4 and significantly increased on day 5. *SNAI1*, *TWIST1*, *ZEB1* (EMT markers), and *CDH1* (MET marker)/*ACTB* were also evaluated using qRT-PCR (Figure S14). (C) *KLF4*, *POU5F1*, and *SOX9* (stemness markers)/*ACTB* expression levels. Compared with their levels on day 0, *POU5F1* and *SOX9* expression levels significantly increased on days 1–5 and days 1–4, while *KLF4* expression only significantly increased on day 5. For qRT-PCR analysis of the genes of interest, the same samples as those used for *ASCL2/ACTB* were used (Figures S2A and S9). Day 0 before the Dox treatment and days 1, 2, 3, 4, and 5 of the culture period after the Dox treatment. Values shown are the means \pm SD ($n=4$). * $P < 0.05$, ** $P < 0.01$. Dox, doxycycline; EMT, epithelial-mesenchymal transition; MET, mesenchymal-epithelial transition; qRT-PCR, quantitative reverse-transcription polymerase chain reaction.

evaluate cell growth, and they showed that ASCL2 expression increased the growth of HepG2 cells while the knockdown decreased the growth of HepG2 and HUH-6 cells. Indeed, the expression of *CCND1* and *MYC*, Wnt signaling pathway target genes^{3,20} increased in HepG2 cells after ASCL2 induction and prior to the upregulation of cell growth and viability, suggesting that ASCL2 promotes growth by upregulating *CCND1* and *MYC* through Wnt signal amplification in HB. Consistent with our results, previous reports on colon cancer (CC) have suggested that ASCL2 increases cell viability and colony-formation ability.^{4,5} One possible explanation for the decrease in *CCND1* and *MYC* expression from day 4 is that ASCL2 is also involved in negative feedback for the Wnt signaling pathway.^{3,21,22}

In the migration and invasion assays, ASCL2 expression increased the mobility of HepG2 cells while the knockdown decreased the mobility of HepG2 and HUH-6 cells. The increased ratio of *SNAI1*, *TWIST1*, and *ZEB1* (EMT markers) in comparison to *CDH1* (MET marker)¹⁶ in HepG2 cells after ASCL2 induction may increase cell migration and invasion by promoting EMT. The results of this study are consistent with those of previous studies on CC and gastric cancer, which suggest that ASCL2 increases cell mobility.⁵⁻⁷ Furthermore, previous studies have reported that the expression of the EMT-related genes *SNAI1*, *TWIST1*, and *ZEB1* fluctuates with the expression of ASCL2.^{5,7} Similarly, with HB, ASCL2 is highly expressed, indicating that EMT-related genes may also be highly expressed, which may subsequently promote EMT and the progression of HB.²

The sphere-formation assays showed that ASCL2 expression increased the stemness of HepG2 cells while the knockdown decreased stemness. These results are consistent with those of previous studies, which suggest that ASCL2 increases the sphere-forming abilities of CC and esophageal cancer cells.⁸⁻¹⁰ Indeed, the expression of the stemness-related genes *KLF4*, *POU5F1*, and *SOX9* increased in HepG2 cells after ASCL2 induction, suggesting that ASCL2 may be an upstream regulator of stemness-related genes and play a role in increasing the stemness of HB. Consistent with our results for stemness-related gene expression, previous studies have reported that ASCL2 regulates stemness-related genes.^{3,9,10} Interestingly, in our study, *POU5F1* and *SOX9* expression increased from day 1 and *KLF4* expression increased only on day 5, which suggests the existence of different regulation mechanisms for ASCL2 target genes.

In the colony-formation assays using 5-aza-dC, ASCL2 expression inhibited the decrease in colony number, suggesting that a combination of DNA demethylation and ASCL2 expression is involved in the aggressive malignant phenotypes of HB. The influence of epigenomic status and ASCL2 expression differs with cancer type. Methylation profiling of 100 and 114 gastric cancers showed that the demethylation of ASCL2 resulted in its upregulation; however, whether the specific hypomethylation was maintained and allowed the sites to bind ASCL2 was not investigated.^{23,24} Methylation profiling of 90 CCs showed that promoter methylation of the Wnt target genes including ASCL2 was a predictor for recurrence.²⁵

Our previous study hypothesized that the “cell of origin in HB” is derived from ASCL2-positive premature hepatoblasts.² The results

from this study show that cell growth and stemness are increased when ASCL2 induces the expression of proliferation- and stemness-related genes, and ASCL2-positive premature hepatoblasts may have high proliferative potential and stemness, similar to intestinal epithelial cells (Figure S19).^{2,3} Hepatoblasts and intestinal epithelial cells are similarly derived from the endoderm. The results of this study further support the hypothesis from our previous study. Additionally, gene expression and array-based comparative genomic hybridization analysis of HB in 85 patients identified two subclasses, one of which was as a highly proliferating immature subclass typified by upregulated *MYC* and stemness-related genes (C2 type).²⁶ ASCL2 regulation of these genes^{3,9,10} indicates that it may be involved in this subclass²⁶ and in the “cell of origin in HB”. In addition, comprehensive transcriptomic characterization of HB in 113 patients using high-throughput technologies identified a new hallmark of HB, the overexpression of 14q32 genes.²⁷ Previous studies have shown that the 14q32 region has a key role in human development and cancer,^{28,29} and a study of fetal liver samples indicated elevated gene expression,²⁶ reinforcing the idea that HB recapitulates the pathological and molecular features of the developing liver.^{26,30} The expression of *MEG3* in the region was increased in HepG2 cells after ASCL2 induction, and ASCL2 may thus be involved in the expression of the long non-coding RNA *MEG3* (a 14q32 gene), an epigenetic regulation via the RNA, and in the “cell of origin in HB” that may recapitulate the features of developing livers.

When compared with cell lines other than the endoderm-derived cells, ASCL2 reportedly influences the malignant potential of breast cancer and Merkel cell carcinoma cell lines, which are ectoderm-derived cells.^{31,32} Consistent with our results, these reports suggest that the upregulation of ASCL2 promotes the proliferation, migration, and invasion of breast cancer cells,³¹ while its downregulation reduces the growth of Merkel cell carcinoma cells.³²

In conclusion, the results of this study suggest that ASCL2 induces the malignant phenotypes of HB, such as growth, mobility, and stemness. To the best of our knowledge, this is the first study to elucidate the relationship between ASCL2 expression and the malignant potential in HB. Our results indicate that ASCL2 is a key factor in the induction of aggressive malignant phenotypes in patients with HB. However, our experiments were limited to in vitro studies. In the future, both in vitro and in vivo studies will be required to confirm our results. Furthermore, although we observed changes in both colony and sphere size as well as cell shape, such as with invadopodia, we did not perform a morphological analysis of the changes. Further investigations will therefore be required to confirm these results. Taken together, this study presents an improved understanding of the detailed role of ASCL2, and this may lead to the discovery of new therapeutic targets for HB.

AUTHOR CONTRIBUTIONS

Yutaka Kato: Conceptualization; data curation; formal analysis; investigation; methodology; project administration; resources; software; validation; visualization; writing – original draft; writing – review and editing. **Takahiro Fukazawa:** Conceptualization; data

curation; formal analysis; funding acquisition; investigation; methodology; project administration; resources; software; validation; writing – review and editing. **Keiji Tanimoto:** Funding acquisition; methodology; resources; software; supervision. **Masami Kanawa:** Resources; supervision. **Masato Kojima:** Resources; writing – review and editing. **Isamu Saeki:** Resources; writing – review and editing. **Sho Kurihara:** Resources; writing – review and editing. **Ryo Touge:** Resources; writing – review and editing. **Nobuyuki Hirohashi:** Resources; software; supervision. **Satoshi Okada:** Resources; supervision; writing – review and editing. **Eiso Hiyama:** Funding acquisition; project administration; resources; software; supervision; writing – review and editing.

ACKNOWLEDGMENTS

We thank Mrs. Yoko Hayashi, Mrs. Shoko Hirano, Dr. Takanori Harada, Dr. Masataka Tsuge, Ms. Chiyo Oda, and Mr. Kengo Mekata at Hiroshima University for their technical support. Part of this study was conducted at the Analysis Center of Life Science, Natural Science Center for Basic Research and Development, Hiroshima University.

FUNDING INFORMATION

This research was partially supported by JSPS KAKENHI (grant numbers JP20K08927, JP22H031315, and JP22KK0133) and by the Japan Agency for Medical Research and Development (AMED; grant numbers JP22ck0106609 and JP22am221403).

CONFLICT OF INTEREST STATEMENT

The authors have no conflicts of interest to declare.

DATA AVAILABILITY STATEMENT

All materials used in this study, as well as the data sets and analyses, are available from the Natural Science Center for Basic Research and Development, Hiroshima University, and can be provided upon reasonable request to the corresponding author.

ETHICS STATEMENT

Approval of the research protocol by an Institutional Reviewer Board: N/A.

Informed Consent: N/A.

Registry and the Registration No. of the study/trial: N/A.

Animal Studies: N/A.

ORCID

Masato Kojima  <https://orcid.org/0000-0001-7783-0289>

Eiso Hiyama  <https://orcid.org/0000-0001-9179-5037>

REFERENCES

- Little MH, Thomson DB, Hayward NK, Smith PJ. Loss of alleles on the short arm of chromosome 11 in a hepatoblastoma from a child with Beckwith-Wiedemann syndrome. *Hum Genet.* 1988;79(2):186-189. doi:10.1007/BF00280564
- Nagae G, Yamamoto S, Fujita M, et al. Genetic and epigenetic basis of hepatoblastoma diversity. *Nat Commun.* 2021;12(1):5423. doi:10.1038/s41467-021-25430-9
- Schuijers J, Junker JP, Mokry M, et al. Ascl2 acts as an R-spondin/Wnt-responsive switch to control stemness in intestinal crypts. *Cell Stem Cell.* 2015;16(2):158-170. doi:10.1016/j.stem.2014.12.006
- Giakountis A, Moulos P, Zarkou V, et al. A positive regulatory loop between a wnt-regulated non-coding RNA and ASCL2 controls intestinal stem cell fate. *Cell Rep.* 2016;15(12):2588-2596. doi:10.1016/j.celrep.2016.05.038
- Tian Y, Pan Q, Shang Y, et al. MicroRNA-200 (miR-200) cluster regulation by achaete scute-like 2 (Ascl2): impact on the epithelial-mesenchymal transition in colon cancer cells. *J Biol Chem.* 2014;289(52):36101-36115. doi:10.1074/jbc.M114.598383
- Shang Y, Chen H, Ye J, Wei X, Liu S, Wang R. HIF-1 α /Ascl2/miR-200b regulatory feedback circuit modulated the epithelial-mesenchymal transition (EMT) in colorectal cancer cells. *Exp Cell Res.* 2017;360(2):243-256. doi:10.1016/j.yexcr.2017.09.014
- Zuo Q, Wang J, Chen C, et al. ASCL2 expression contributes to gastric tumor migration and invasion by downregulating miR223 and inducing EMT. *Mol Med Rep.* 2018;18(4):3751-3759. doi:10.3892/mmr.2018.9363
- Zhao R, Quaroni L, Casson AG. Identification and characterization of stemlike cells in human esophageal adenocarcinoma and normal epithelial cell lines. *J Thorac Cardiovasc Surg.* 2012;144(5):1192-1199. doi:10.1016/j.jtcvs.2012.08.008
- Wei X, Ye J, Shang Y, et al. Ascl2 activation by YAP1/KLF5 ensures the self-renewability of colon cancer progenitor cells. *Oncotarget.* 2017;8(65):109301-109318. doi:10.18632/oncotarget.22673
- Ye J, Liu S, Shang Y, Chen H, Wang R. R-spondin1/Wnt-enhanced Ascl2 autoregulation controls the self-renewal of colorectal cancer progenitor cells. *Cell Cycle.* 2018;17(8):1014-1025. doi:10.1080/15384101.2018.1469874
- Jubb AM, Chalasani S, Frantz GD, et al. Achaete-scute like 2 (ascl2) is a target of Wnt signalling and is upregulated in intestinal neoplasia. *Oncogene.* 2006;25:3445-3457. doi:10.1038/sj.onc.1209382
- Yuan YF, Wang JP, Li JQ, et al. Frequent epigenetic inactivation of spleen tyrosine kinase gene in human hepatocellular carcinoma. *Clin Cancer Res.* 2006;12(22):6687-6695. doi:10.1158/1078-0432.CCR-06-0921
- Tao SF, Zhang CS, Guo XL, et al. Anti-tumor effect of 5-aza-2'-deoxycytidine by inhibiting telomerase activity in hepatocellular carcinoma cells. *World J Gastroenterol.* 2012;18(19):2334-2343. doi:10.3748/wjg.v18.i19.2334
- Kanda T, Tada M, Imazeki F, Yokosuka O, Nagao K, Saisho H. 5-aza-2'-deoxycytidine sensitizes hepatoma and pancreatic cancer cell lines. *Oncol Rep.* 2005;14(4):975-979. doi:10.3892/or.14.4.975
- Fukazawa T, Tanimoto K, Shrestha L, et al. Simulated microgravity enhances CDDP-induced apoptosis signal via p53-independent mechanisms in cancer cells. *PLOS ONE.* 2019;14(7):e0219363. doi:10.1371/journal.pone.0219363
- Tanabe S, Aoyagi K, Yokozaki H, Sasaki H. Gene expression signatures for identifying diffuse-type gastric cancer associated with epithelial-mesenchymal transition. *Int J Oncol.* 2014;44(6):1955-1970. doi:10.3892/ijo.2014.2387
- Kallio PJ, Pongratz I, Gradin K, McGuire J, Poellinger L. Activation of hypoxia-inducible factor 1 α : posttranscriptional regulation and conformational change by recruitment of the Arnt transcription factor. *Proc Natl Acad Sci USA.* 1997;94(11):5667-5672. doi:10.1073/pnas.94.11.5667
- Buachan P, Chularojmontri L, Wattanapitayakul SK. Selected activities of *Citrus maxima* Merr. Fruits on human endothelial cells: enhancing cell migration and delaying cellular aging. *Nutrients.* 2014;6(4):1618-1634. doi:10.3390/nu6041618

19. Nafie E, Lolarga J, Lam B, et al. Harmine inhibits breast cancer cell migration and invasion by inducing the degradation of Twist1. *PLOS ONE*. 2021;16(2):e0247652. doi:10.1371/journal.pone.0247652
20. Gödeke J, Maier S, Eichenmüller M, Müller-Höcker J, von Schweinitz D, Kappler R. Epigallocatechin-3-gallate inhibits hepatoblastoma growth by reactivating the Wnt inhibitor SFRP1. *Nutr Cancer*. 2013;65(8):1200-1207. doi:10.1080/01635581.2013.828085
21. Barker N, Tan S, Clevers H. Lgr proteins in epithelial stem cell biology. *Development*. 2013;140(12):2484-2494. doi:10.1242/dev.083113
22. Wieck MM, Schlieve CR, Thornton ME, et al. Prolonged absence of mechanoluminal stimulation in human intestine alters the transcriptome and intestinal stem cell niche. *Cell Mol Gastroenterol Hepatol*. 2017;3(3):367-388.e1. doi:10.1016/j.jcmgh.2016.12.008
23. Wang K, Yuen ST, Xu J, et al. Whole-genome sequencing and comprehensive molecular profiling identify new driver mutations in gastric cancer. *Nat Genet*. 2014;46(6):573-582. doi:10.1038/ng.2983
24. Kwon OH, Park JL, Baek SJ, et al. Aberrant upregulation of ASCL2 by promoter demethylation promotes the growth and resistance to 5-fluorouracil of gastric cancer cells. *Cancer Sci*. 2013;104:391-397. doi:10.1111/cas.12076
25. de Sousa EMF, Colak S, Buikhuisen J, et al. Methylation of cancer-stem-cell-associated Wnt target genes predicts poor prognosis in colorectal cancer patients. *Cell Stem Cell*. 2011;9:476-485. doi:10.1016/j.stem.2011.10.008
26. Cairo S, Armengol C, De Reyniès A, et al. Hepatic stem-like phenotype and interplay of Wnt/beta-catenin and Myc signaling in aggressive childhood liver cancer. *Cancer Cell*. 2008;14(6):471-484. doi:10.1016/j.ccr.2008.11.002
27. Carrillo-Reixach J, Torrens L, Simon-Coma M, et al. Epigenetic footprint enables molecular risk stratification of hepatoblastoma with clinical implications. *J Hepatol*. 2020;73(2):328-341. doi:10.1016/j.jhep.2020.03.025
28. Da Rocha ST, Edwards CA, Ito M, Ogata T, Ferguson-Smith AC. Genomic imprinting at the mammalian Dlk1-Dio3 domain. *Trends Genet*. 2008;24(6):306-316. doi:10.1016/j.tig.2008.03.011
29. Benetatos L, Hatzimichael E, Londin E, et al. The microRNAs within the DLK1-DIO3 genomic region: involvement in disease pathogenesis. *Cell Mol Life Sci*. 2013;70(5):795-814. doi:10.1007/s00018-012-1080-8
30. Zimmermann A. The emerging family of hepatoblastoma tumours: from ontogenesis to oncogenesis. *Eur J Cancer*. 2005;41(11):1503-1514. doi:10.1016/j.ejca.2005.02.035
31. Han S, Jin X, Hu T, Chi F. ARHGAP25 suppresses the development of breast cancer by an ARHGAP25/Wnt/ASCL2 feedback loop. *Carcinogenesis*. 2023;44(5):369-382. doi:10.1093/carcin/bgad042
32. Park DE, Cheng J, McGrath JP, et al. Merkel cell polyomavirus activates LSD1-mediated blockade of non-canonical BAF to regulate transformation and tumorigenesis. *Nat Cell Biol*. 2020;22(5):603-615. doi:10.1038/s41556-020-0503-2

SUPPORTING INFORMATION

Additional supporting information can be found online in the Supporting Information section at the end of this article.

How to cite this article: Kato Y, Fukazawa T, Tanimoto K, et al. Achaete-scute family bHLH transcription factor 2 activation promotes hepatoblastoma progression. *Cancer Sci*. 2024;00:1-12. doi:10.1111/cas.16051